

# Green Synthesis of UV-Reactive Polycarbonates from Levoglucosenone and 5-Hydroxymethyl Furfural

Aihemaiti Kayishaer, Mattia Annatelli, Chloe M Hansom, Louis M. M. Mouterde, Aurélien A. M. Peru, Fabio Aricò,\* Florent Allais,\* and Sami Fadlallah\*

This study focuses on the synthesis of fully renewable polycarbonates (PCs) starting from cellulose-based platform molecules levoglucosenone (LGO) and 2,5-bis(hydroxymethyl)furan (BHMF). These unique bio-based PCs are obtained through the reaction of a citronellol-containing triol (Triol-citro) derived from LGO, with a dimethyl carbonate derivative of BHMF (BHMF-DC). Solvent-free polymerizations are targeted to minimize waste generation and promote an eco-friendly approach with a favorable environmental factor (E-factor). The choice of metal catalyst during polymerization significantly influences the polymer properties, resulting in high molecular weight (up to 755 kDa) when  $\text{Na}_2\text{CO}_3$  is employed as an inexpensive catalyst. Characterization using nuclear magnetic resonance confirms the successful incorporation of the furan ring and the retention of the terminal double bond of the citronellol pendant chain. Furthermore, under UV irradiation, the presence of both citronellol and furanic moieties induces singular structural changes, triggering the formation of three distinct structures within the polymer network, a phenomenon herein occurs for the first time in this type of polymer. These findings pave the way to new functional materials prepared from renewable monomers with tunable properties.

the “mindful” utilization of renewable raw materials, like biomass-derived platform molecules, has emerged as a highly promising approach.<sup>[3,4]</sup> Among the diverse biomass-based building blocks,<sup>[5]</sup> levoglucosenone (LGO)<sup>[6]</sup> and 5-hydroxymethyl furfural (HMF)<sup>[7]</sup> have garnered significant attention for their abundance and their potential to be transformed into high-performing materials, such as polycarbonates (PCs).<sup>[8]</sup>

Recently, LGO has been introduced as a versatile chiral platform for synthesizing partially and fully renewable monomers and polymers.<sup>[9]</sup> Among the diverse reported LGO monomers,<sup>[10–15]</sup> Triol-citro<sup>[16]</sup> has demonstrated good reactivity with dimethoxycarbonyl isosorbide (DCI) derived from isosorbide<sup>[17]</sup> (Scheme 1). Isosorbide has gained prominence as a glucose-derived platform molecule in the synthesis of a wide range of biobased polymers, including PCs.<sup>[18]</sup> Its unique properties, including rigidity and non-toxicity, make it a commercially available and cost-effective choice for producing alternative polymers.

This aspect aligns with one of the significant challenges in the biobased polymer industry: balancing cost-efficiency with the production of polymers that match the performance of their fossil fuel counterparts. In this context, the  $\text{Cs}_2\text{CO}_3$ -mediated preparation of citronellol-containing PC was achieved. The resulting PC, named PC-DCI, had a number average molecular weight ( $M_n$ ) of up to 23.4 kDa when polymerization was conducted in bulk.<sup>[19]</sup> However, when Cyrene was employed as a reaction medium, the  $M_n$  reached an impressive 682 kDa. Nevertheless, using solvents like Cyrene comes with drawbacks, such as tedious solvent removal and increased waste generation.<sup>[20]</sup> As previously depicted, Cyrene contributed up to 93% of the total waste generated in the polymerization process.<sup>[10]</sup>

On the other hand, the bifunctional aromatic molecule HMF presents a valuable building block offering numerous compounds with diverse applications (Scheme 2).<sup>[21]</sup> Among these, 2,5-bis(hydroxymethyl)furan (BHMF) and the corresponding dimethyl carbonate derivative (BHMF-DC), stand out as promising derivatives of HMF.<sup>[7]</sup> The conversion of HMF to diols, exemplified by compounds such as BHMF, offers a multitude of notable advantages. First and foremost, this conversion is simple, cost-effective, environmentally friendly, safe, and reliable.<sup>[22]</sup>

## 1. Introduction

The principles of green chemistry play a crucial role in our quest for sustainable materials. These guidelines are not only aimed at reducing reliance on fossil-based resources but also at minimizing waste generation in production processes.<sup>[1,2]</sup> As a result,

A. Kayishaer, C. M Hansom, L. M. M. Mouterde, A. A. M. Peru, F. Allais, S. Fadlallah

URD Agro-Biotechnologies Industrielles (ABI)  
CEBB

AgroParisTech, 3 Rue des Rouges-Terres, Pomacle 51110, France  
E-mail: florent.allais@agroparistech.fr; sami.fadlallah@agroparistech.fr

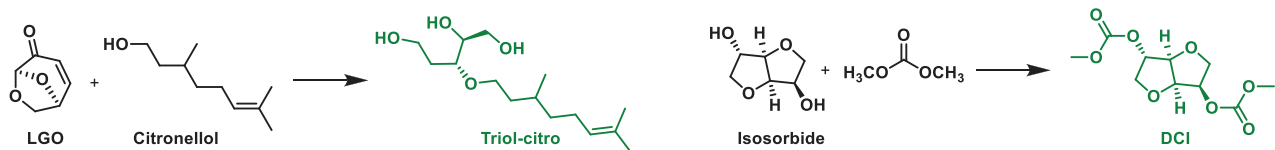
M. Annatelli, F. Aricò  
Department of Environmental Sciences  
Informatics and Statistics

Ca' Foscari University of Venice  
Via Torino 155, Venezia, Mestre 30172, Italy  
E-mail: fabio.arico@unive.it

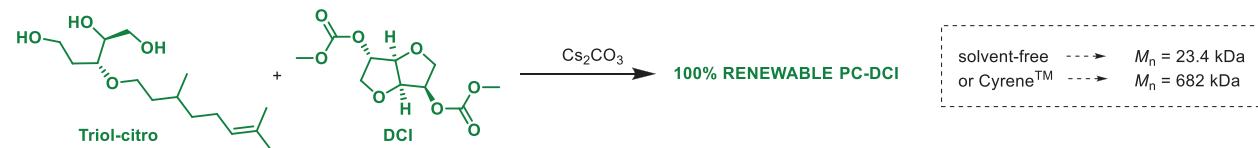
 The ORCID identification number(s) for the author(s) of this article can be found under <https://doi.org/10.1002/marc.202300483>

DOI: 10.1002/marc.202300483

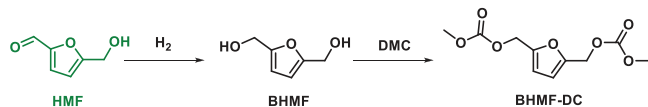
## A) Monomers synthesis



## B) Polycarbonate synthesis



**Scheme 1.** Synthesis of citronellol-containing PC-DCI from Triol-citro and DCI.



**Scheme 2.** A selection of promising derivatives of HMF.

In addition, BHMF plays an essential role as a versatile chemical intermediate, serving as the starting molecule for the synthesis of a variety of important compounds, including dicarbonate monomers and dienes.<sup>[23]</sup> In addition to their role as intermediates, they also serve as essential monomers in the polyester industry. Thus, these furan-based building blocks from HMF can play a central role in the polymer industry, particularly in terms of sustainability and environmental impact.<sup>[23]</sup> However, despite their promise, their intrinsic thermodynamic instability often results in side reactions, especially during polycondensation reactions. This leads to the formation of numerous side products,<sup>[24]</sup> such as oligomers along with unwanted humins.<sup>[7]</sup> To pave the way for a more efficient and sustainable synthesis of HMF and BHMF, further research and development are essential.<sup>[25]</sup> Addressing these challenges will also involve finding compatible co-monomers and polymerization conditions to achieve the controlled production of 100% renewable polycarbonates with desired properties such as high molecular weights.

Building upon prior research efforts,<sup>[19]</sup> the present study seeks to broaden the range of sustainable PCs by introducing a novel combination of Triol-citro and BHMF-DC. Based on the emerging platform molecules LGO and HMF, exceptionally high molecular weight PCs with the citronellol function are synthesized “in bulk”. It should be also mentioned that to the best of our knowledge, this is the first time that BHMF-DC has been effectively used as a monomer for a bio-based polymer. By embracing green chemistry principles and sustainable practices, this innovative combination not only enhances the versatility of resulting polymer structures but also paves the way for the development of eco-friendly, multifunctional materials with tailor-made properties. Additionally, a particularly intriguing aspect is the simultaneous presence of the furan ring and the citronellol moiety, which exhibited exceptional behavior under UV irradiation, rendering the resulting PCs amenable to further functionalization. This is another feature that distinguishes the

current study from previous research on PC-DCI polymers,<sup>[19]</sup> where only the photocrosslinkable citronellol moiety was present. The inclusion of both components opens up exciting possibilities for further exploration in the realm of sustainable materials.

## 2. Results and Discussion

Considering the thermal stability of BHMF-DC, which degrades  $\approx 128$  °C (Figure S33, Supporting Information) with a melting temperature of  $\approx 85$  °C (Figure S25, Supporting Information), we carefully selected the polymerization procedure not only to prevent degradation of the starting materials during the initial stages but also to attain polymers with high  $M_n$  values. Polycondensation experiments reported in Table 1 involved a sequential three-step process. Carefully adjusting the temperature at each step allowed to balance between stabilizing intermediates in the initial phase and promoting polymerization in the final product. First, we aimed to obtain more stable macromonomers (or oligomers) by reacting the selected monomers in the presence of a catalyst at 100 °C for 18 h under  $N_2$  atmosphere. Then, the temperature was gradually increased to 160 °C for 3 h with continuous stirring to initiate the polymerization of the stable intermediates. Finally, in the third step, the temperature was raised to 220 °C under vacuum for 2 h to facilitate the removal of any remaining volatile components and helps finalize the polymerization process. (Scheme 3).

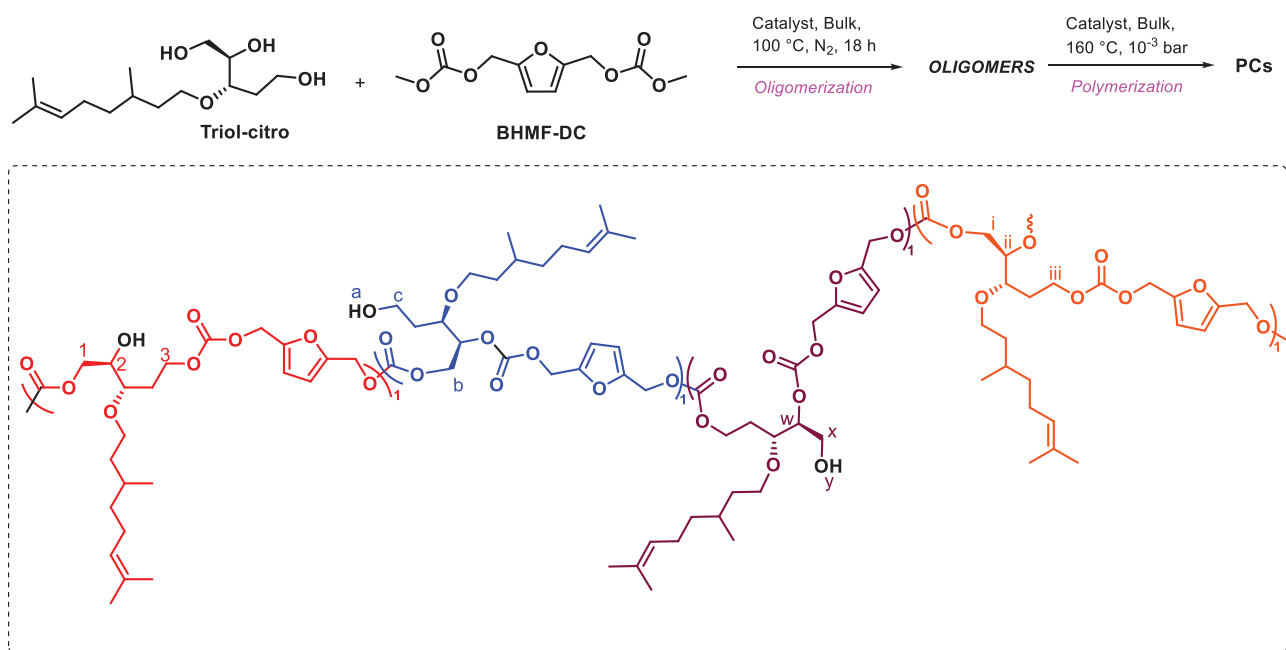
### 2.1. Catalyst Screening

To promote the polymerization reaction, 2 mol% of various metal-based catalysts, including  $Cs_2CO_3$ ,  $Li_2CO_3$ ,  $K_2CO_3$ ,  $Na_2CO_3$ ,  $LiAcac$ , and  $Ti(OBu)_4$ , were screened. Our catalyst selection was influenced by recent studies conducted by Shin et al.<sup>[26]</sup> and by our work,<sup>[19]</sup> which demonstrated that the nature of the (alkali) metal significantly impacts the preparation and properties of isosorbide-derived polycarbonates. An alkali metal acetylacetone ( $LiAcac$ ) was also selected, based on the exceptional activity reported by Zheng et al.<sup>[27]</sup> in the preparation of isosorbide-based homo- and co-polycarbonates compared to  $Ti(OBu)_4$  and  $Zn(OAc)_2$ .

**Table 1.** Polycondensation of Triol-citro and BHMF-DC.

Run#	Sample	Catalyst <sup>a)</sup>	Yield [%] <sup>b)</sup>	$M_n$ [kDa] <sup>c)</sup>	$D^c)$	$T_g$ [°C] <sup>d)</sup>	$T_{d5\%}$ [°C] <sup>e)</sup>	$T_{d50\%}$ [°C] <sup>e)</sup>	E-factor <sup>f)</sup>
1	PC-Cs	$Cs_2CO_3$	83	23	1.65	-50	146	277	0.22
2	PC-Li	$Li_2CO_3$	78	671	1.05	-46	173	276	0.29
3	PC-K	$K_2CO_3$	70	734	1.09	-47	175	309	0.46
4	PC-Na	$Na_2CO_3$	75	755	1.05	-48	197	324	0.34
5	PC-LiAc	LiAcac	73	716	1.06	-44	176	315	0.38
6	PC-Ti	$Ti(OBu)_4$	84	161	1.39	-33	152	306	0.20

<sup>a)</sup> 2 mol% of catalyst; <sup>b)</sup> Isolated yield of the crude product, %yield = (isolated mass/theoretical mass) × 100; <sup>c)</sup> Determined in DMF (10 mM LiBr) at 50 °C, calibration was performed with poly(methyl methacrylate) standards; <sup>d)</sup> Glass transition temperature determined by DSC, third heating step, temperature ramp 10 °C min<sup>-1</sup>; <sup>e)</sup> TGA degradation temperature at which 5% ( $T_{d5\%}$ ) or 50% ( $T_{d50\%}$ ) mass loss was observed under nitrogen, temperature ramp 10 °C min<sup>-1</sup>; <sup>f)</sup> E factor<sup>[28]</sup> =  $\frac{m(\text{Triol-citro}) + m(\text{BHMF-DC}) + m(\text{catalyst}) - m(\text{polymer})}{m(\text{polymer})}$ .

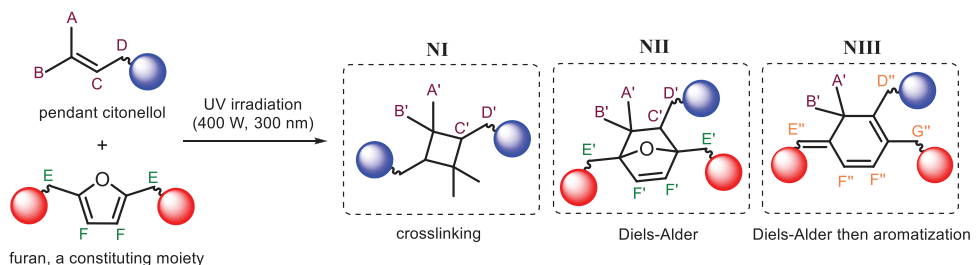
**Scheme 3.** Schematic representation of a potential PC structure synthesized through one-pot bulk polycondensation of Triol-citro and BHMF-DC.

Using  $Cs_2CO_3$  as a catalyst resulted in an  $M_n$  value of 23 kDa, which is comparable to the 23.4 kDa obtained when DCI was used as a co-monomer.<sup>[19]</sup> Additionally, differential scanning calorimetry (DSC) and thermogravimetric analysis (TGA) showed comparable results, with a low glass transition temperature ( $T_g$ ) of -50 °C and thermal stability ( $T_{d5\%}$  and  $T_{d50\%}$ ) of 146 and 277 °C, respectively. However, a surprising increase in  $M_n$  was observed when  $Na_2CO_3$  was employed as a promoter. The resulting bio-based PC had the highest  $M_n$  value (755 kDa) achieved in this investigation, as well as the highest  $T_{d5\%}$  (197 °C) and  $T_{d50\%}$  (324 °C). Except for the polycondensation conducted in the presence of  $Ti(OBu)_4$ , close  $T_g$  values were obtained for all polymers reported in Table 1.

Several factors might contribute to this unexpected increase in  $M_n$ . The distinct reactivity of furan-based monomers, the unique catalyst-triol-furan interactions, and the potential or not for branching, could contribute to distinct polymer chain growth and molecular weights. Additionally, varying catalyst-substrate

interactions might also influence catalytic performance and selectivity, further influencing the polymerization outcome. For example, in the case of PC-DCI polymers,<sup>[19]</sup> we found that using a solvent like Cyrene at monomer concentration of 2 M in the presence of  $Cs_2CO_3$ , resulted in a peak at 9.86 min in size exclusion chromatography (SEC) analysis, corresponding to a polymer with an  $M_n$  of 682.2 kDa. The difference in  $M_n$  between polymers synthesized in solution versus bulk (see Scheme 1) was attributed to better homogenization of the reaction mixture and enhanced solubility of both the metal catalyst and the produced oligomers/polymers.<sup>[19,26]</sup>

In the present study, it is worth noting that solution polymerization using Cyrene was also explored leading to similar results compared to bulk polymerization, with the exception of  $Cs_2CO_3$ . However, since solvents contribute significantly to the overall waste generated in chemical/polymerization processes (evidenced by entry 7 in Table S1, Supporting Information), we decided to primarily focus on bulk polymerization. This



**Scheme 4.** Schematic representation of the UV-induced crosslinking and structural changes.

approach led to significantly lower E-factors,<sup>[28,29]</sup> ranging from 0.22 to 0.46 kg of waste/kg, in contrast to an E-factor of 240 kg of waste/kg of product observed in the production of PC-DCI,<sup>[19]</sup> with an  $M_n$  of 682.2 kDa, using Cyrene as a solvent.

Haut du formulaire  
Bas du formulaire

## 2.2. Structural Characterization

In previous experiments,<sup>[19]</sup> we found that the presence and type of catalyst significantly influenced the polymer composition, leading to either linear or/and dendritic structures. For example, without a catalyst, the polymerization resulted in PCs with mostly 99% linear units and only 1% of dendritic structures (Dq). However, when using  $\text{Cs}_2\text{CO}_3$  as a catalyst (2 mol%), Dq reached 47%. Unfortunately, in the present work, the impact of the metal catalyst on the polymer microstructure could not be monitored through different nuclear magnetic resonance (NMR) techniques due to the complexity of both attributing and/or differentiating the peaks of the constituent units. Scheme 3 is a simplified representation illustrating a potential structure that may arise from the polycondensation of the three hydroxyls of Triol-citro and two carbonates of BHMF-DC. Nonetheless,  $^1\text{H}$  NMR analysis of the crude product clearly confirmed the successful polycondensation reaction between the hydroxyl groups of Triol-citro and carbonates of BHMF-DC (see Figures S7–S11, Supporting Information for more information). The presence of the aromatic furan ring was examined using  $^1\text{H}$  NMR (at 6.55–6.20 ppm) and  $^{13}\text{C}$  NMR (at 1.53–1.55 ppm). Similar to isosorbide-based polymers,<sup>[19]</sup> the PC structures showed multiple carbonyl peaks (156–154 ppm), attributed to the distinct reactivity of functional groups participating in the polycondensation. The terminal double bond of the pendant citronellol moiety remained intact in the polymer structure, as confirmed by the peak at 5.07 ppm in  $^1\text{H}$  NMR and the single carbon peak at 125 ppm.

## 2.3. UV-Induced Crosslinking and Structural Changes

To mitigate solubility issues after UV reaction, PC-Cs (#1) was consciously selected for its low molecular weight, thus also optimizing the efficiency of UV-induced crosslinking (Scheme 4). We monitored the evolution of UV-mediated structural changes using  $^1\text{H}$  NMR (Figure 1). As the exposure time increased, we observed the  $\text{C}=\text{CH}$  peak ( $\text{H}_C$ ) of citronellol at 5.07 ppm gradually disappearing, while  $\text{H}_C$  at 2.07 ppm emerged, demonstrating C–C bond formation and leading to cyclobutene (NI) via photo-induced (2 + 2) cyclization (Scheme 4). This also

resulted in the transformation of protons  $\text{H}_D$  and  $\text{H}_A$  at 1.92 and 1.56 ppm to  $\text{H}_{D'}$  and  $\text{H}_{A'}$  at 1.63 and 1.20 ppm, respectively. Similar results were obtained for the previously reported DCI-based polymers.<sup>[19]</sup> However, in this case study, the presence of furan rings in UV-irradiated samples, resulted in additional structural changes.

Careful examination revealed the formation of another structure (NII) due to UV-mediated Diels–Alder reaction<sup>[30]</sup> of the furan ring with the double bond of citronellol, leading to a rearrangement of the double bond as depicted in Scheme 4. This new structure exhibited characteristic peaks at 4.59 and 5.51 ppm ( $\text{H}_{E''}$  and  $\text{H}_{F''}$ ) and resulted in the disappearance of  $\text{H}_F$  at 6.66–5.95 ppm and  $\text{H}_E$  at 5.10 ppm. Additionally, new peaks at 8.12, 7.10–7.00, 4.86, and 3.16 ppm emerged. We hypothesized the formation of a third structure (NIII) where the double bond is localized outside the ring. This can be supported by the appearance of deshielded proton  $\text{H}_{E''}$  at 8.12 ppm due to the presence of neighboring oxygen and double bond. The protons  $\text{H}_{F''}$ ,  $\text{H}_{G''}$ , and  $\text{H}_{D''}$  at 7.10–7.00, 4.86, and 3.16 ppm, respectively, further validated this structure. To our knowledge, such UV-triggered formation of such three structures in the same polymer network has not been reported previously.

Indeed, furan derivatives, such as 2-methylfuran (MF), 2,5-dimethylfuran (DMF), furfural (FF), HMF, as well as various alkenes/alkynes, have been studied for their ability to undergo Diels–Alder cycloaddition reactions followed by aromatization.<sup>[30]</sup> In classical aromatization reactions, a cyclic intermediate is formed, characterized by alternating single and double bonds, ultimately leading to the formation of a fully conjugated aromatic system (NV, Scheme 5). However, the presence of terminal two methyl groups in the case of citronellol prevents the formation of the expected aromatic compound due to the inability of the carbon to coordinate five bonds in its valence shell. As a result, we hypothesized a reorganization of the cyclic intermediate, which potentially leads to the formation of a partially aromatic compound (NIII) as shown by the assumed mechanism in Scheme 5.

DSC analysis revealed an increase in  $T_g$  from  $-50$  to  $-19$  °C after UV irradiation of PC-Cs for 7 h. As the crosslinking degree increased, the network chains' mobility decreased, leading to a less flexible and more rigid structure with a higher  $T_g$  value. TGA analysis was also performed to assess the impact of photo-induced reactions on thermal stability, showing a significant increase from 277 to 383 °C after UV irradiation. The TGA thermogram displayed a two-profile degradation (Figure S32, Supporting Information), supporting the presence of various structural compositions.

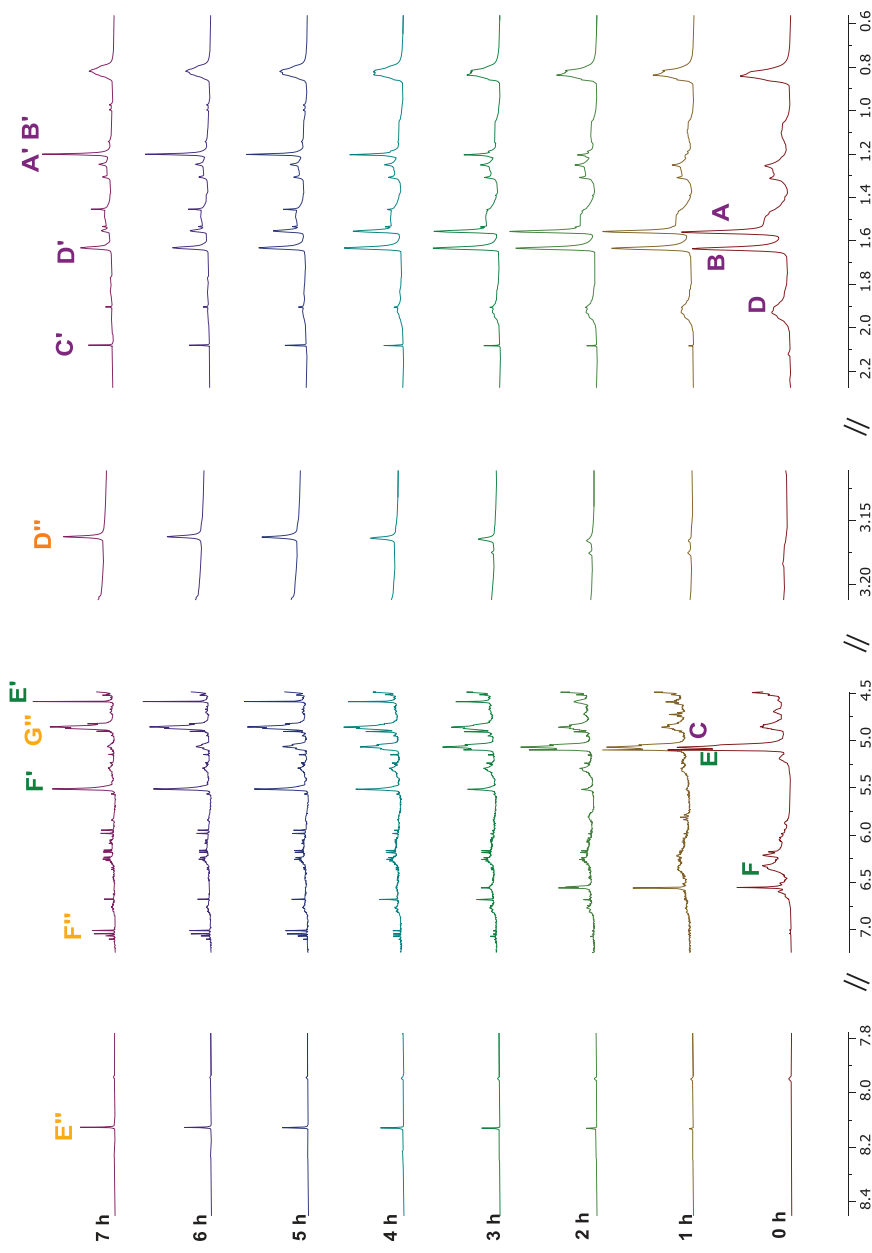
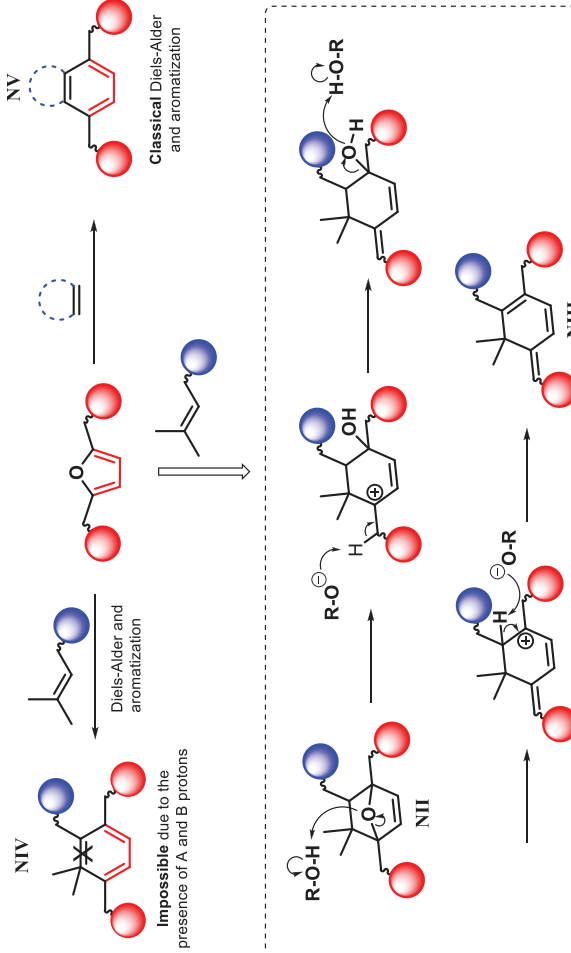
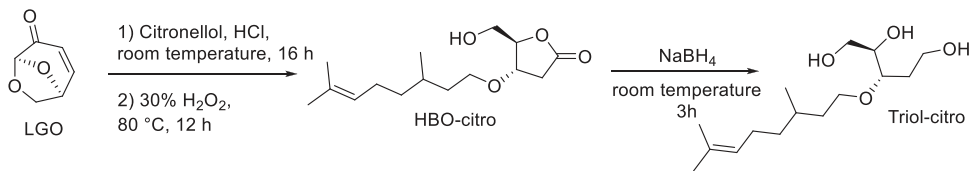


Figure 1. Monitoring of  $^1\text{H}$  NMR (DMSO- $d_6$ ) spectra of a PC-CCs after exposure to UV irradiation (400 W, 300 nm) for 0–7 h.



Scheme 5. Assumed mechanism of the conversion of BCMF-DC polymer units into NIII.



**Scheme 6.** Synthesis of Triol-citro from LGO.

### 3. Conclusion

In conclusion, the investigation of LGO-furanic-based polycarbonates has yielded new intriguing and significant findings. The choice of metal catalysts has a profound impact on polymer compositions, resulting in unexpectedly high  $M_n$  polymers synthesized in bulk. Our focus on bulk polymerization has led to a more environmentally friendly approach with minimized waste generation. However, further research is needed to fully comprehend the underlying mechanisms behind this unusual behavior. Additionally, the presence of furanic moieties in the polymer backbone has introduced novel structural changes under UV irradiation. The UV-triggered formation of three distinct structures within the same polymer network is remarkable. This opens up exciting possibilities for future applications in fields like tissue engineering and wound healing, thanks in particular to the low glass transition temperatures of the resulting polymer. As our understanding of these unique polymer structures deepens, future studies can explore their potential applications and optimize their properties for various industrial uses.

### 4. Experimental Section

**Chemical and Reagents:** Levoglucosenone was graciously provided by the Circa group. Citronellol (Sigma-Aldrich), sodium borohydride >98% (Sigma-Aldrich), dimethyl carbonate (Sigma-Aldrich), titanium(IV) butoxide 99+% (Fisher), cesium carbonate 99.5% (Fisher), lithium carbonate 99.99% (Fisher), potassium carbonate 99% (Sigma-Aldrich), sodium carbonate (VWR), Lithium acetylacetone (TCI). HPLC grade solvents were purchased from ThermoFisher Scientific and used as received. NMR solvents including  $\text{CDCl}_3$  and  $\text{DMSO}-d_6$  were purchased from Cambridge Isotopes Laboratories. Ultra-pure laboratory-grade water was obtained from MilliQ, 18.2 megaOhms. TLC analyses were performed on an aluminum strip coated with Silica Gel 60 F254 from Merck, revealed under UV light (254 nm) then in the presence of potassium permanganate staining solution. All manipulations with air-sensitive chemicals were performed using standard Schlenk techniques on a dual-manifold line.

**Characterization: Nuclear Magnetic Resonance (NMR) Spectroscopy:**  $^1\text{H}$  NMR spectra were recorded on a Bruker Fourier 300 MHz ( $\text{CDCl}_3$  residual signal at 7.26 ppm and  $\text{DMSO}-d_6$  residual signal at 2.5 ppm).  $^{13}\text{C}$  NMR spectra were recorded on a Bruker Fourier 300 (75 MHz) ( $\text{CDCl}_3$  residual signal at 77.16 ppm and  $\text{DMSO}-d_6$  residual signal at 39.52 ppm). Data were reported as follows: chemical shift ( $\delta$  ppm), assignment. All NMR assignments were also made using  $^1\text{H}$ - $^1\text{H}$  COSY,  $^1\text{H}$ - $^{13}\text{C}$  HMBC, and  $^1\text{H}$ - $^{13}\text{C}$  HSQC spectra.

**Size exclusion chromatography (SEC):** It was performed at 50 °C using an Agilent Technologies 1260 Infinity Series liquid chromatography system with an internal differential refractive index detector, a viscometer detector, a laser, and two PLgel columns (5  $\mu\text{m}$  MIXED-D 300  $\times$  7.5 mm) using 10 mM Lithium Bromide in HPLC grade dimethylformamide as the mobile phase at a flow rate of 1.0 mL min $^{-1}$ . Calibration was performed with poly(methyl methacrylate) standards from Agilent Technologies.

**Thermogravimetric Analysis (TGA):** It was measured with a TGA Q500 (TA Instruments). Typically,  $\approx$ 2 mg of each sample was equilibrated at 50 °C for 30 min and was flushed with highly pure nitrogen gas. All the

experiments were performed with a heating rate of 10 °C min $^{-1}$  up to 500 °C. The reported values of  $T_{d5\%}$  and  $T_{d50\%}$  represented the temperature at which 5% and 50% of the mass is lost, respectively. Concerning the normalization of TGA, a slight shift in some cases took place during the isothermal step at 50 °C which was necessary to stabilize the sample in the oven prior to analysis. The corresponding degradation temperatures reported in this manuscript considered this slight shift while calculating  $T_{d5\%}$  and  $T_{d50\%}$  of the reported polymers.

**Differential Scanning Calorimetry (DSC):** It was performed with a DSC Q20 (TA Instruments). Typically,  $\approx$ 8 mg sample was placed in a sealed pan, flushed with highly pure nitrogen gas, and passed through a heat-cool-heat cycle at 10 °C min $^{-1}$  in a temperature range of  $-80$  to 120 °C. Three heat/cool cycles were done for each sample, where the last two cycles were dedicated to analyzing the heat flow of the sample after being cooled in controlled conditions. The  $T_g$  values recorded herein were those obtained from the third cycle.

**Fourier-transform infrared spectroscopy (FTIR):** It was recorded on a Cary 630 FTIR Spectrometer by Agilent (Wilmington, DE, USA).

**Synthesis of Monomers: HBO-citro (Scheme 6):** A biphasic mixture of LGO (50 g, 0.4 mol), citronellol (512 mL, 1.8 mol), and HCl (5 N, 0.6 mol) was stirred at room temperature for 16 h. The resulting mixture was cooled down with an ice bath followed by the dropwise addition of a 30% solution of  $\text{H}_2\text{O}_2$  (2 mL) for 2 h (Scheme 6).<sup>[16]</sup> After completion of the addition, the reaction was heated up to 80 °C and stirred for 12 h. The presence of  $\text{H}_2\text{O}_2$  was evaluated with peroxide strips and, if any, the residual  $\text{H}_2\text{O}_2$  was quenched using sodium sulfite. The reaction was extracted with ethyl acetate (two times). Organic layers were washed with brine, dried over anhydrous  $\text{MgSO}_4$ , filtered, and evaporated to dryness. This step was followed by distillation to remove excess citronellol. The crude product was purified by flash chromatography (gradient 90/10 to 20/80, cyclohexane/ethyl acetate as eluent) to give 62 g of HBO-citro as a pale-yellow oil (58%).

$^1\text{H}$  NMR ( $\delta$  ppm,  $\text{CDCl}_3$ ): 5.01 (broad t,  $J$  = 5.19 Hz, 1H,  $\text{H}_{13}$ ), 4.43 (s, 1H,  $\text{H}_3$ ), 4.11 (d,  $J$  = 7.0 Hz, 1H, OH), 3.84 (dd,  $J$  = 3.3 and 12.4 Hz, 1H,  $\text{H}_4$ ), 3.65 (dd,  $J$  = 3.3 and 12.4 Hz, 2H,  $\text{H}_2$ ), 3.39 (m, 2H,  $\text{H}_7$ ), 2.81 (dd,  $J$  = 7.0 and 18.1 Hz, 1H,  $\text{H}_{5a}$ ), 2.44 (dd,  $J$  = 3.3 and 18.1 Hz, 1H,  $\text{H}_{5b}$ ), 1.90 (m, 2H,  $\text{H}_{12}$ ), 1.61 (s, 3H,  $\text{H}_{15}$ ), 1.53 (s, 3H,  $\text{H}_{16}$ ), 1.27–1.07 (m, 4H,  $\text{H}_{11}$ ,  $\text{H}_8$ ), 0.82 (d,  $J$  = 6.4 Hz, 3H,  $\text{H}_{10}$ );  $^{13}\text{C}$  NMR ( $\delta$  ppm,  $\text{CDCl}_3$ ): 176.7 ( $\text{C}_6$ ), 131.2 ( $\text{C}_{14}$ ), 124.6 ( $\text{C}_{13}$ ), 85.9 ( $\text{C}_3$ ), 76.1 ( $\text{C}_4$ ), 67.6 ( $\text{C}_7$ ), 62.1 ( $\text{C}_2$ ), 37.1 ( $\text{C}_{11}$ ), 36.5 ( $\text{C}_8$ ), 35.9 ( $\text{C}_5$ ), 29.3 ( $\text{C}_9$ ), 25.7 ( $\text{C}_{15}$ ), 25.3 ( $\text{C}_{12}$ ), 19.4 ( $\text{C}_{10}$ ), 17.6 ( $\text{C}_{16}$ ).

**Triol-Citro (Scheme 6):** An aqueous solution of sodium borohydride (1.14 g in 3 mL of water, 30 mmol) was added dropwise to a solution of HBO-citro (4.5 g, 15 mmol) in THF (60 mL) in a water-ice bath. The reaction mixture was stirred at room temperature for 3 h. The reaction was quenched with acetone and a 20% aqueous solution of citric acid (20 mL). The reaction was extracted twice with ethyl acetate. Organic layers were washed with brine, dried over anhydrous magnesium sulfate, filtered, and evaporated to dryness. The crude product was purified by flash chromatography (gradient 90/10 to 20/80, cyclohexane/ethyl acetate as eluent) to give 3.39 g of Triol-citro as a colorless oil (82%).

$^1\text{H}$  NMR ( $\delta$  ppm,  $\text{DMSO}-d_6$ ): 5.07 (t,  $J$  = 7.2 Hz, 1H,  $\text{H}_{15}$ ), 4.55 (s, OH), 4.38 (s, OH), 4.34 (s, OH), 3.50–3.27 (broad, m, 8H,  $\text{H}_9$ ,  $\text{H}_7$ ,  $\text{H}_5$ ,  $\text{H}_4$ ,  $\text{H}_2$ ), 1.93 (broad, m, 2H,  $\text{H}_{14}$ ), 1.64 (s, 3H,  $\text{H}_{17}$ ), 1.56 (s, 3H,  $\text{H}_{18}$ ), 1.50–1.10 (broad, m, 5H,  $\text{H}_{13}$ ,  $\text{H}_{11}$ ,  $\text{H}_{10}$ ), 0.84 (d,  $J$  = 6.2 Hz, 3H,  $\text{H}_{12}$ );  $^{13}\text{C}$  NMR ( $\delta$  ppm,  $\text{DMSO}-d_6$ ): 130.8 ( $\text{C}_{16}$ ), 125.1 ( $\text{C}_{15}$ ), 77.7 ( $\text{C}_5$ ), 73.5 ( $\text{C}_4$ ), 67.9 ( $\text{C}_9$ ), 63.4 ( $\text{C}_2$ ), 58.2 ( $\text{C}_7$ ), 37.3 ( $\text{C}_{13}$ ), 37.1 ( $\text{C}_{10}$ ), 33.9 ( $\text{C}_6$ ), 29.2 ( $\text{C}_{11}$ ), 25.9 ( $\text{C}_{17}$ ), 25.4 ( $\text{C}_{14}$ ), 19.8 ( $\text{C}_{12}$ ), 17.9 ( $\text{C}_{18}$ ).

**BHMF-DC:** To a solution of BHMF (0.5 g, 3.90 mmol) in dimethyl carbonate (6–30 eq. mol), potassium carbonate (2.0 eq. mol) was added

and the mixture was allowed to react under stirring at 90 °C for 16 h. Then, the mixture was filtered, and the solvent evaporated under a vacuum. The pure compound was isolated as a yellow solid with an 87% yield.

<sup>1</sup>H NMR ( $\delta$  ppm, DMSO-*d*<sub>6</sub>): 6.56 (S, 2H, H<sub>5</sub>, H<sub>6</sub>), 5.11 (S, 4H, H<sub>3</sub>, H<sub>8</sub>), 3.72 (S, 6H, H<sub>1</sub>, H<sub>10</sub>); <sup>13</sup>C NMR ( $\delta$  ppm, DMSO-*d*<sub>6</sub>): 154.86 (C<sub>2</sub>, C<sub>9</sub>), 149.78 (C<sub>4</sub>, C<sub>7</sub>), 112.25 (C<sub>5</sub>, C<sub>6</sub>), 60.85 (C<sub>3</sub>, C<sub>8</sub>), 54.87 (C<sub>1</sub>, C<sub>10</sub>).

**Polymerization of Triol-Citro and BHMF-DC:** A typical melt polycondensation experiment (#1, Table S1, Supporting Information) was performed as follows. Under N<sub>2</sub> atmosphere, Triol-citro (250 mg, 0.911 mmol), furan-2,5-diylbis(methylene) dimethyl bis(carbonate) (334 mg, 1.366 mmol) and 2 mol% of metal-catalyst (cesium carbonate) based on Triol-citro were added into a 10 mL round-bottom flask connected to a vacuum line, equipped with a condensate trap. The reaction mixture was heated from room temperature to 100 °C at a heating rate of  $\approx$ 32 °C/5 min and stirred continuously at 400 rpm for 18 h. Then the temperature was gradually increased to 160 °C. After 3 h of stirring the temperature was further increased to 220 °C and a high vacuum (10<sup>-3</sup> bar) was then applied for 2 h. The obtained polymer was dried at ambient temperature for 48 h. The NMR (DMSO-*d*<sub>6</sub>) spectra of the polycarbonate obtained are provided in Figures S7–S11 (Supporting Information).

**UV Crosslinking Experiment:** PC-Cs (#1, Table S1, Supporting Information) was crosslinked using a 400 W source of UV irradiation (300 nm) in a Rayonet Photochemical Reactor. A 200 mg sample was UV irradiated for 1, 2, 3, 4, 5, 6, and 7 h. A few mgs were taken for each time point to analyze the crosslinked polymers by <sup>1</sup>H NMR. The crosslinked material was then analyzed by DSC and TGA.

## Supporting Information

Supporting Information is available from the Wiley Online Library or from the author.

## Acknowledgements

A.K. and M.A. contributed equally to this work. The authors are grateful to the Circa group for its generous gift of LGO, and to Grand Reims, Département de la Marne, and Grand Est region for financial support. This article was also within the frame of COST Action FUR4Sustain (CA18220–European network of FURan-based chemicals and materials FOR a Sustainable development), supported by COST (European Cooperation in Science and Technology). Chloe M Hansom thanks the National Science Foundation (NSF) for its support through the REU program (NSF CHE-2244028).

## Conflict of Interest

The authors declare no conflict of interest.

## Data Availability Statement

The data that support the findings of this study are available in the supplementary material of this article.

## Keywords

aromatization, Diels–Alder, green chemistry, photo-crosslinking, post-polymerization modification, sustainable polymers

Received: August 10, 2023

Revised: October 5, 2023

Published online: November 3, 2023

- [1] K. N. Ganesh, D. Zhang, S. J. Miller, K. Rossen, P. J. Chirik, M. C. Kozlowski, J. B. Zimmerman, B. W. Brooks, P. E. Savage, D. T. Allen, A. M. Voutchkova-Kostal, *Org. Process Res. Dev.* **2021**, *25*, 1455.
- [2] P. Anastas, N. Eghbali, *Chem. Soc. Rev.* **2009**, *39*, 301.
- [3] S. Fadlallah, P. Sinha Roy, G. Garnier, K. Saito, F. Allais, *Green Chem.* **2021**, *23*, 1495.
- [4] H. El Itawi, S. Fadlallah, F. Allais, P. Perré, *Green Chem.* **2022**, *24*, 4237.
- [5] T. J. Farmer, M. Mascal, in *Introduction to Chemicals from Biomass*, John Wiley & Sons, Ltd, Chichester, West Sussex **2015**, pp. 89–155.
- [6] M. B. Comba, Y.-H. Tsai, A. M. Sarotti, M. I. Mangione, A. G. Suárez, R. A. Spanevello, *Eur. J. Org. Chem.* **2018**, *2018*, 590.
- [7] G. Trapasso, G. Mazzi, B. Chicharo, M. Annatelli, D. Dalla Torre, F. Aricò, *Org. Process Res. Dev.* **2022**, *26*, 2830.
- [8] B. Y. Karlinskii, V. P. Ananikov, *Chem. Soc. Rev.* **2023**, *52*, 836.
- [9] S. Fadlallah, L. M. M. Mouterde, G. Garnier, K. Saito, F. Allais, *Sustainability & Green Polymer Chemistry Volume 2: Biocatalysis and Biobased Polymers*, American Chemical Society, Washington, DC, **2020**, pp. 77–97.
- [10] S. Fadlallah, A. A. M. Peru, L. Longé, F. Allais, *Polym. Chem.* **2020**, *11*, 7471.
- [11] S. Fadlallah, A. L. Flourat, L. M. M. Mouterde, M. Annatelli, A. A. M. Peru, A. Gallos, F. Aricò, F. Allais, *Macromol. Rapid Commun.* **2021**, *42*, 2100284.
- [12] F. Diot-Néant, L. Mouterde, S. Fadlallah, S. A. Miller, F. Allais, *ChemSusChem* **2020**, *13*, 2613.
- [13] C. M. Warne, S. Fadlallah, A. C. Whitwood, J. Sherwood, L. M. M. Mouterde, F. Allais, G. M. Guebitz, C. R. McElroy, A. Pellis, *Green Chem.* **2023**, *16*, 2154573.
- [14] S. Fadlallah, A. A. M. Peru, A. L. Flourat, F. Allais, *Eur. Polym. J.* **2020**, *138*, 109980.
- [15] S. Fadlallah, Q. Carboué, L. M. M. Mouterde, A. Kayishaer, Y. Werghi, A. A. M. Peru, M. Lopez, F. Allais, *Polymers* **2022**, *14*, 2082.
- [16] A. Kayishaer, S. Fadlallah, L. M. M. Mouterde, A. A. M. Peru, Y. Werghi, F. Brunois, Q. Carboué, M. Lopez, F. Allais, *Molecules* **2021**, *26*, 7672.
- [17] M. Annatelli, D. Dalla Torre, M. Musolino, F. Aricò, *Catal. Sci. Technol.* **2021**, *11*, 3411.
- [18] M. D. Zenner, Y. Xia, J. S. Chen, M. R. Kessler, *ChemSusChem* **2013**, *6*, 1182.
- [19] S. Fadlallah, A. Kayishaer, M. Annatelli, L. M. M. Mouterde, A. A. M. Peru, F. Aricò, F. Allais, *Green Chem.* **2022**, *24*, 2871.
- [20] F. P. Byrne, S. Jin, G. Paggiola, T. H. M. Petchey, J. H. Clark, T. J. Farmer, A. J. Hunt, C. Robert McElroy, J. Sherwood, *Sustainable Chem. Processes* **2016**, *4*, 7.
- [21] Q.-S. Kong, X.-L. Li, H.-J. Xu, Y. Fu, *FPT* **2020**, *209*, 106528.
- [22] A. G. Sathicq, M. Annatelli, I. Abdullah, G. Romanelli, F. Aricò, *Sustainable Chem. Pharm.* **2021**, *19*, 100352.
- [23] C. Post, D. Maniar, V. S. D. Voet, R. Folkersma, K. Loos, *ACS Omega* **2023**, *8*, 8991.
- [24] M. Annatelli, G. Trapasso, D. D. Torre, L. Pietrobon, D. Redolfi-Bristol, F. Aricò, *Adv. Sustainable Syst.* **2022**, *6*, 2200297.
- [25] M. G. Davidson, S. Elgie, S. Parsons, T. J. Young, *Green Chem.* **2021**, *23*, 3154.
- [26] Y. S. Eo, H.-W. Rhee, S. Shin, *J. Ind. Eng. Chem.* **2016**, *37*, 42.
- [27] Q. Li, W. Zhu, C. Li, G. Guan, D. Zhang, Y. Xiao, L. Zheng, *J. Polym. Sci., Part A: Polym. Chem.* **2013**, *51*, 1387.
- [28] R. A. Sheldon, *Green Chem.* **2017**, *19*, 18.
- [29] R. A. Sheldon, *ACS Sustainable Chem. Eng.* **2018**, *6*, 32.
- [30] Z. Li, Y. Jiang, Y. Li, H. Zhang, H. Li, S. Yang, *Catal. Sci. Technol.* **2022**, *12*, 1902.